NASA
Technical Memorandum 100583

USAAVSCOM
Technical Memorandum 88-B-010

Improvements to Tilt Rotor Performance Through Passive Blade Twist Control

Mark W. Nixon

April 1988

National Aeronautics and
Space Administration

Langley Research Center
Hampton, Virginia 23665

United States Army
Aviation Systems
Command

Aviation R&T Activity

Summary

A passive blade twist control concept is presented in which the twist distribution of a tilt rotor blade is elastically changed as a function of rotor speed. The elastic twist deformation is used to achieve two different blade twist distributions corresponding to the two rotor speeds used on conventional tilt rotors in hover and forward flight. By changing the blade twist distribution, the aerodynamic performance can be improved in both modes of flight. The concept presented in this paper obtains a change in twist distribution with extension-twist-coupled composite blade structure. This investigation first determines the linear twists which are optimum for each flight mode. Based on the optimum linear twist distributions, three extension-twist-coupled blade designs are developed using coupled-beam and laminate analyses integrated with an optimization analysis. The designs are optimized for maximum twist deformation subject to material strength limitations. The aerodynamic performances of the final designs are determined which show that the passive blade twist control concept is viable, and can enhance conventional tilt rotor performance.

Introduction

The most unique feature of a tilt rotor aircraft is its wingtip-mounted rotors which are directed to a vertical position in hover, but are tilted to a horizontal position in forward flight. Clearly, the design of a tilt rotor requires technologies which are traditional to both helicopters and fixed-wing aircraft. The overlapping of these technologies leads to design compromises because there is no solution which is optimum for both flight regimes. One such compromise exists in the twist design of a tilt-rotor blade. Typically, a tilt-rotor blade is designed with a twist distribution which produces acceptable hover performance at the cost of a lower forward flight propulsive efficiency.

The aerodynamic performance of tilt rotor aircraft would be improved if blade twist could be tailored to the requirements of both hover and forward flight. The twist distributions which are optimum for each flight condition, under the assumption of uniform inflow, are presented in reference 1. The two distributions are significantly different which suggests that there is a performance improvement to be gained through a twist change between the flight modes. However, no actual performance values are reported in reference 1. A more sophisticated twist optimization study was performed in reference 2. Here, a two-piece linear twist variation was used to approximate the non-linear twist used on a conventional metal blade of the XV-15. An optimum twist was determined for forward flight performance which improved propulsive efficiency by about 5 percent. A twist variation study for hover was also performed in reference 2. However, because the analysis assumed uniform inflow, the results showed little sensitivity to twist selection. Further investigation is required to determine an optimum twist design and its resulting performance benefits for the hover condition. This is because references 1 and 2 both use uniform inflow theory which is generally not sufficient for predicting hover performance trends.

The concept of changing blade twist between two flight modes can be realized with the use of composite rotor blades, designed to exhibit extension-twist coupling through an arrangement of off-axis ply angles and stacking sequences. In forward flight, the rotor speed of a typical tilt rotor is 20 percent less than it is in hover. Thus, there is a net change in centrifugal forces which can be used to passively obtain the desired rotor blade twist for each flight mode. The extent of the improvement in aerodynamic performance depends on how closely the actual twist developed in hover and forward flight approaches the optimum twist in each of the two modes. This in turn depends on the magnitude of twist deformation which can be produced within the material strength limits of the blade structure. As the allowable twist deformation increases, so does the ability to obtain desirable twist distributions in both modes of flight. Although the desired twist change occurs for a 20 percent change in rotational velocity, it is the twist change caused by increasing rotational velocity from zero to its maximum value which produces the maximum blade stresses. For structural substantiation of a design, the centrifugally generated stresses must be considered simultaneously with bending stresses resulting from air and inertia loads.

In reference 3, passive twist control concepts are applied to the extension-twist-coupled design of a rotor blade for the XV-15 tilt rotor assuming a 15 percent change in operating rpm between hover and forward flight. The design was first required to match the baseline XV-15 composite blade in flapwise and lead-lag bending stiffnesses, torsional stiffness, chordwise *c.g.* location, and mass distribution per unit span. Using these requirements only about 0.5° twist change was developed. A second design study was performed which allowed deviations from the baseline XV-15 blade in the bending and torsional stiffnesses, but retained the baseline mass distribution and *c.g.* location. This resulted in a 2° twist change over the same 15 percent rpm range. The approach used in reference 3 was to alter an existing conventional design. It is likely that larger twist changes can be developed if blades are designed using both mass and stiffness to take full advantage of extension-twist-coupling benefits. An indication that larger twist changes can be obtained is found in reference 4. Here, composite tube tests resulted in twist rates of between 0.384 and 0.487 deg/in. at the material strength design-limits for structures representative of rotor blade spars. This translates to about 48 degrees of total twist for the tailorable span of the XV-15 tilt-rotor blade. However, the single cell structure tested in reference 4 was not completely representative of an actual blade cross section, and was also not subjected to simultaneous bending loads. Thus, the twist deformation which can be obtained within material strength limitations when all applicable loads are considered remains in question.

The purpose of this paper is to show that passive blade twist control through use of an extension-twist-coupled structural design is a feasible concept for tilt rotor blades. The investigation described in this report addresses the aerodynamic and structural aspects of a passive twist-control rotor blade system. First, the aerodynamically-optimum twist distributions are determined for hover and

forward flight. The performance benefits gained from use of these twists over the twist employed in the conventional XV-15 blade are also ascertained. Three extension-twist-coupled designs are then developed, based on a D-shape spar and a NACA-0012 airfoil, with the intent of achieving aerodynamically-improved twist distributions. For this design study the maximum twist deformation available at 100 percent rpm, subject to material strength limitations, is determined using a coupled-beam analysis and a laminate analysis integrated with an optimization analysis. The twist deformations available to each design are used to obtain twist distributions which improve the performance associated with the conventional XV-15 blade twist in both hover and forward flight.

Nomenclature

c	chord length, in.
$c.g.$	center of gravity location, in.
C_T	coefficient of Thrust, $\frac{T}{\rho\pi R^2(\omega R)^2}$
E_{11}	lamina longitudinal modulus, psi
E_{22}	lamina transverse modulus, psi
G_{12}	lamina shear modulus, psi
HP_{min}	minimum horsepower required
r	radial position from center of rotation, in.
R	radius, in.
S	Lamina shear strength, ksi
T	Thrust, lb
T_{rt}	spar thickness in root section, in.
T_{sk}	airfoil skin thickness, in.
T_{tr}	spar thickness in transition section, in.
T_{tw}	spar thickness in twisting section, in.
v_0	velocity of the wake at rotor disk, ft/sec
V	free stream velocity, ft/sec
$wnsm$	weight of non-structural mass, lb/in
$wtip$	tip weight, lb
x, y, z	principal coordinate directions
X	lamina strength in the fiber direction, ksi
Y	lamina strength in the matrix direction, ksi
α	general ply angle, deg
α_{opt}	optimum angle of attack, deg
α_{sk}	laminate fiber angle in airfoil skin, deg
α_{sp}	laminate fiber angle in spar, deg
$\Delta 20$	twist deformation at tip between 80 and 100% rpm, deg
$\Delta 80$	twist deformation at tip between 0 and 80% rpm, deg
$\Delta 100$	twist deformation at tip between 0 and 100% rpm, deg
Δx_{tr}	length of transition section, in.
Δx_{tw}	length of twisting section, in.
θ	blade twist angle, deg
μ	tip-speed ratio, $\frac{V}{\omega R}$
ν	inflow velocity, ft/sec
ν_{12}	lamina primary Poisson ratio
ρ	density of air, slug/ft^3
ω	rotational velocity, rad/sec

Subscripts

n	number of repetitions of a lamina sequence
s	make lamina symmetrical

Aerodynamic Considerations

The aerodynamic part of this investigation focuses on determining the rotor blade twist distributions which are optimum for aerodynamic performance in hover and forward flight. The twist distributions which are optimum under the assumption of uniform inflow are presented first. Next, optimum twists with linear distributions are determined for each flight mode using proven analysis techniques. The performance associated with the optimum linear twists are compared to the performance associated with the twist used on the conventional XV-15 tilt rotor blade and the twists which are optimum based on uniform inflow. Finally, the process of twist distribution selection in practical extension-twist-coupled designs is explained.

Optimum Twist for Uniform Inflow

For a rotor blade operating in a free-stream with the rotational plane perpendicular to the flow direction (uniform inflow), the optimum performance is realized when the blade twist distribution is such that the Betz condition is satisfied. The Betz condition states that the trailing vortex sheet moves aft as a rigid helical sheet, which is to say that the wake displacement velocity is radially constant (refs. 1 and 5). Using combined blade element/momentum theory to satisfy the Betz condition, reference 1 shows that the displacement velocity of the vortex wake can be approximated by

$$v_0 = \frac{\omega R}{2}\left(\sqrt{\mu^2 + 2C_T} - \mu\right) \tag{1}$$

and the optimum blade twist distribution is given by

$$\theta = \tan^{-1}\left(\frac{v_0}{\omega r} + \mu\frac{R}{r}\right) + \alpha_{opt} \tag{2}$$

In hover, μ is zero, and the wake displacement velocity v_0 is the same as the induced velocity ν so that equation 1 reduces to

$$\nu = \omega R\sqrt{C_T/2} \tag{3}$$

and equation 2 becomes

$$\theta = \tan^{-1}\left(\frac{\nu}{\omega r}\right) + \alpha_{opt} \tag{4}$$

For a radially constant chord and airfoil section, α_{opt} can be ignored because it is the same for all radial points and, therefore, does not influence the built-in twist distribution. Assuming a radially constant chord and airfoil section, the twist distributions are calculated using equations 2 and 4, and are shown in figure 1. The forward flight twist is shown to be nearly linear with about -42° of twist from root (r/R=.15) to tip. The twist distribution in hover is shown to be highly nonlinear, and has less overall twist, measured root to tip, than the forward flight twist. Conventional tilt-rotor blade twist distributions are designed by interpolating between the optimum hover and optimum forward flight twist distributions. To illustrate this, the conventional XV-15 tilt rotor twist distribution is also plotted in figure 1.

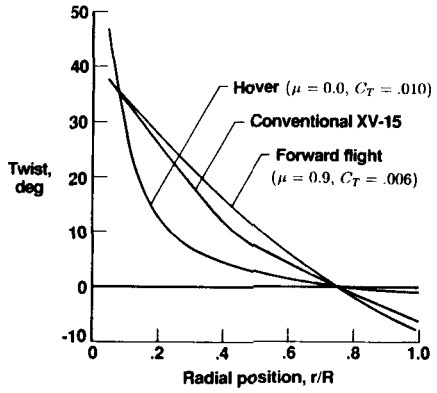

Figure 1. Twist distributions based on uniform inflow.

Optimum Linear Twist Distributions

For this investigation more sophisticated analysis techniques were employed to compute the aerodynamic performance associated with various linear twists. Linear twist distributions were considered because they are easily quantified, and are more commonly used in practice than nonlinear twist distributions. The Comprehensive Analytical Model of Rotorcraft Aerodynamics and Dynamics (CAMRAD, ref. 6) was used to compute performances in the forward flight condition. The hover performances were assessed using HOVT, a strip theory momentum analysis with a nonuniform inflow model, which is based on equations found in reference 7. The hover performance predictions of HOVT have been verified for three different blade designs through correlation with experiments performed at the Langley 4 x 7 meter wind tunnel (ref. 8).

The performance of several linear twists were determined for hover and forward flight using HOVT and CAMRAD, respectively. The aerodynamic blade model used in the analyses was a high-speed 350-knot blade configuration. The performance trends are illustrated in figure 2, where the performance is expressed as a percentage increase in horsepower required over the minimum horsepower required in each flight mode. The minimum horsepower required corresponds to the optimum linear twists which are shown to be -20° in hover and -42° in forward flight. The results of figure 2 also indicate that use of a single compromised linear twist results in an increase in power-required for both modes of flight. The -42° linear twist, found to be optimum for forward flight, is geometrically equivalent to the twist distribution defined by equation 2 which is based on uniform inflow. The forward flight performance associated with the -42° linear twist and the conventional XV-15 twist are compared in figure 3. The -42° linear twist is shown to reduce horsepower required by 6.5 percent at the design velocity. The hover performance was calculated assuming nonuniform inflow for three twist distributions: the conventional XV-15 twist, the uniform-inflow twist defined by equation 4, and the -20° linear twist. The performance results are compared in figure 4 which illustrates that the hover performance associated with the twist based on uniform inflow is worse than the -20° linear twist (based on nonuniform inflow). This is expected because the aerodynamics of the hover condition are highly influenced by the inflow distribution, and in the actual case the inflow is not uniform. Figure 4 also shows that the hover performance can be improved 6.1 percent at the design gross weight by using the -20° linear twist instead of the conventional XV-

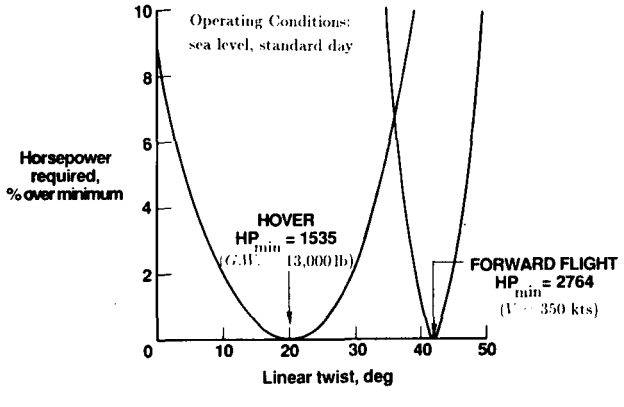

Figure 2. Optimum linear twist distributions for a typical tilt rotor in hover and forward flight.

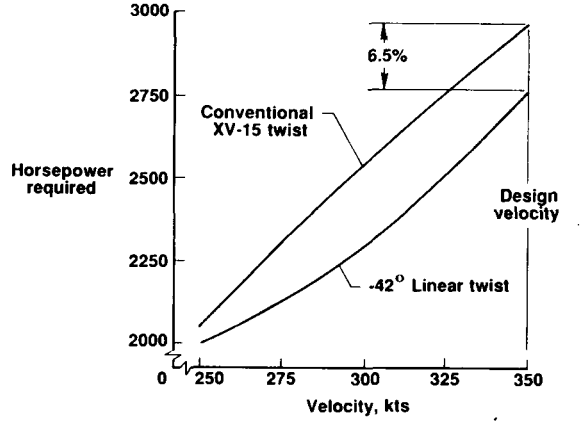

Figure 3. Comparison of forward flight performance for two blade twist distributions.

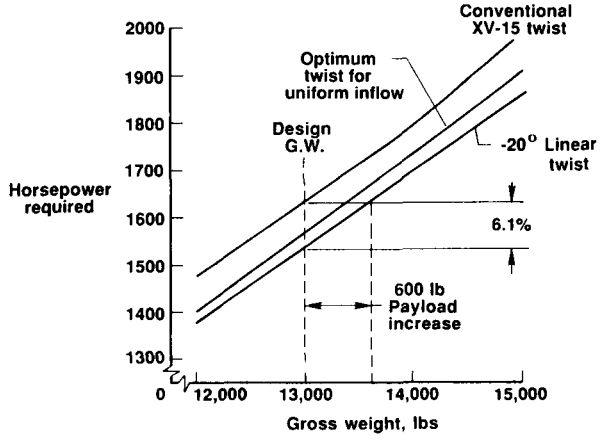

Figure 4. Comparison of hover performance for three blade twist distributions.

15 twist. The figure shows further that the performance benefit can be traded for a 600 lb increase in payload carrying capability. Based on the results of the hover and forward flight predictions, the aerodynamic performance of tilt rotors can be significantly improved if two different linear blade twist distributions are generated, approaching -42° in forward flight and -20° in hover.

Selection of Twist Distribution

The linear twists which were shown to be optimum for hover and forward flight can not both be obtained using the extension-twist-coupled blade concept. The centrifugal forces are a nonlinear function of the rotational velocity so that the twist deformation produced between two radial positions changes nonlinearly with rotor speed. Thus, when using an extension-twist-coupled blade, only one of the tilt rotor flight modes can be specified to have a linear twist distribution. Figure 2 shows that performance in the forward flight condition is much more sensitive to variations in twist selection. Thus, it is advantageous to use the optimum linear twist for forward flight in the forward flight mode which requires use of a nonlinear twist in hover. If a linear twist of -42° is assumed in forward flight at 80 percent rpm then the twist distribution in hover at 100 percent rpm is a nonlinear variation of the desired -20° linear twist.

Assuming a -42° linear twist in forward flight, the nonlinear twist distribution obtained in hover is a function of the particular extension-twist coupled design. The shape of the twist distribution in hover is roughly the same for all practical extension-twist designs because the twist distribution is controlled by the blade weight distribution. The weight distribution cannot, in practice, be altered so much that a significant change in the shape of the twist distribution will occur over a 20 percent change in rotor speed. However, a combination of weight and laminate design can be used to significantly alter the overall magnitude of twist change measured between the blade root and the tip. The magnitude of twist between root and tip has a large influence on the hover performance, but it is not clear what magnitude is optimum. The linear twist study indicates that a twist of -20° is optimum for a linear distribution in hover, but the magnitude of twist desired for a nonlinear distribution may be different.

For the concept of twist control presented in this investigation, the -42° forward flight twist distribution is obtained by determining the twist distribution of the nonrotating, undeformed blade (sometimes referred to as the jig-shape) required for a particular extension-twist-coupled design. The twist deformation at various radial positions are determined for a change in rotational velocity between 0 and 80 percent rpm. These twist deformations are subtracted from the distribution desired in forward flight to obtain the twist distribution necessary for the jig-shape. The twist distribution for the blade in hover is calculated by a similar procedure. In this case, the twist deformation at various radial positions are determined for a change in rotational velocity between 0 and 100 percent rpm. These deformations are then added to the twist distribution of the jig-shape to obtain the twist distribution in hover.

Structural Considerations

Geometry and Materials

The structural blade model used in this design study is based on a 20-inch chord NACA-0012 airfoil with a D-shaped spar. The basic cross-sectional dimensions and components are illustrated in figure 5. The spar and airfoil skin are composed entirely of Ciba-Geigy IM6/R6376 graphite/epoxy laminates. The properties of this material are given in Table I. The blade planform is assumed to be rectangular and to consist of three sections as illustrated in figure 6. Each section is further divided into a series of beam segments for analytical purposes; two in the root section, eight in the transition section, and ten in the twisting section.

The root section extends from the center of rotation to $0.15R$. This section is not extension-twist-coupled and consists only of a spar which is used to represent the hub and built-up root-end blade structure typical of rotor blades. The plies of the laminates in this section are all oriented at 0° to the spanwise axis. Conversely, the spar in the twisting section consists only of off-axis plies. Its laminate is assumed to be of the form $[(\alpha/\alpha + 90)_s]_n$. The transition section is necessary to change laminates from 0° in the root section to an off-axis angle in the twisting section. Thus, the spar in the transition section consists of both 0° and off-axis plies. The layup used in this section is given by $[(\alpha/\alpha + 90/0/90)_s]_n$. The transition section experiences twist deformation, but to a lesser degree than the twisting section because the 0° plies significantly increase the extensional stiffness of the blade. The airfoil skin surrounds the D-spar in both the transition and twisting sec-

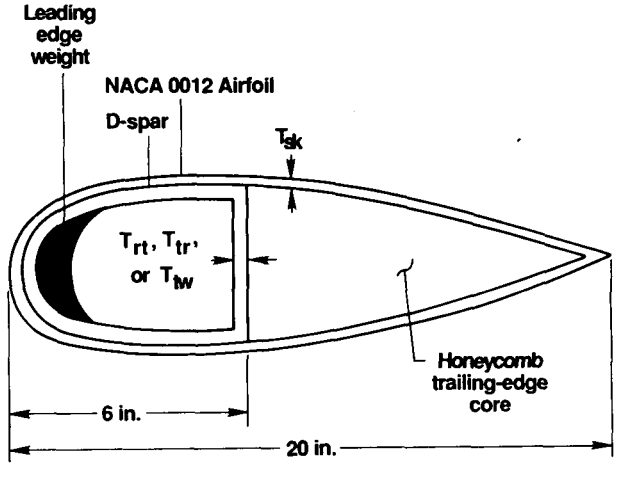

Figure 5. Cross section of the structural model.

Table I. Material Properties of IM6/R6376.

E_{11} (psi x 10^{-6})	E_{22} (psi x 10^{-6})	G_{12} (psi x 10^{-6})	ν_{12}	X (ksi)	Y (ksi)	S (ksi)
23.1	1.4	.76	.34	261.	7.1	11.9

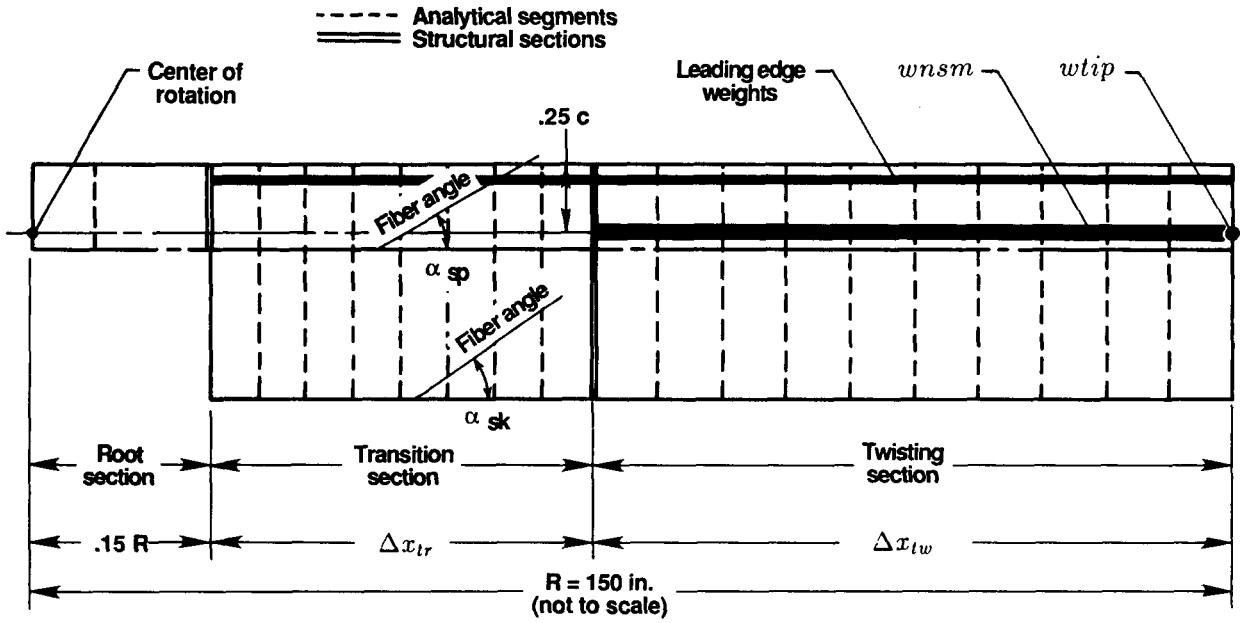

Figure 6. Planform of the structural model.

tions, and is composed of the same type of laminate used in the spar of the twisting section, although α is not necessarily the same for both. The extension-twist-coupled laminates, $[(\alpha/\alpha+90)_s]_n$ and $[(\alpha/\alpha+90/0/90)_s]_n$, are used because elastic coupling can be obtained without thermal coupling. Thermal coupling is avoided when a symmetric laminate is composed entirely of sets of 0/90 plies even if some sets of the 0/90 plies are oriented off-axis. Thus, the laminates used in this structural model produce a twist deformation under an axial load, but do not produce a twist deformation with a change in temperature.

Design Parameters

Several design parameters are used to perform the extension-twist-coupled blade design study. The parameters, T_{tw}, T_{tr}, and T_{rt} are used to control the thicknesses of the D-spar laminates in the twisting, transition, and root sections, respectively. T_{sk} is used to control the thickness of the airfoil skin. The angles of the off-axis plies used in the D-spar of the transition and twisting sections are identical, but may differ from the angle used in the airfoil skin. Thus, α_{sp} controls the off-axis ply angles in the spar, and α_{sk} controls the off-axis ply angles in the airfoil skin. The length of the twisting section is given by the parameter Δx_{tw}. The length of the transition section, Δx_{tr}, is calculated by subtracting the root and twisting section lengths from the blade radius, R. The remaining parameters required for the design study are used to control weight. The tip weight, *wtip*, is assumed to be lumped spanwise at R. The parameter *wnsm* is nonstructural weight per unit span added to the running-weight (weight per unit span) of the twisting section. All of the thickness design parameters are illustrated in figure 5 while the remaining parameters are illustrated in figure 6.

The calculation of blade running-weight is extremely important in this design study because the centrifugal loads result from these weights. Thus, the twist deformation produced at a given rotational velocity is directly related to the running-weight. The running-weights of each section are calculated from the existing design parameters. First, the weight per unit span of each blade section is determined from the corresponding values of T_{sk}, T_{tw}, T_{tr}, and T_{rt}. More running-weight is added to a segment by assuming that the trailing edge core is filled with honeycomb, and that the entire cross section is balanced at the quarter chord with leading-edge weights. Additional weight per unit span may be added to the twisting section by the parameter *wnsm* which is assumed to be placed at the quarter chord. This parameter is used to increase the centrifugal loads when those resulting from the tip weight and other running-weight are not sufficient to create twist deformations which approach the limits of the material strength.

Structural Substantiation

One design condition which is necessary to meet is that a positive margin of safety must be obtained everywhere in the structure when subjected to the substantiating load condition. To insure conservative predictions of the blade strength, the substantiating load condition is composed of the maximum flapwise and inplane bending loads, combined with the maximum centrifugal load, even though all of these loads will not likely be maximum simultaneously. The resulting stresses are used to calculate margins of safety which, for structural substantiation, must be greater than zero everywhere on the structure.

The general procedure for determining the substantiating loads for helicopter rotor blades is outlined in refer-

ence 9. However, this procedure is not completely applicable to the tilt rotor case because the loads produced in the approach of reference 9 account for loads produced in some helicopter maneuvers which are not performed by tilt rotor aircraft. Thus, the maximum bending loads used in this design exercise were obtained from test data on conventional XV-15 rotor blades. The loads on an XV-15 tilt rotor model were determined from wind tunnel tests and are reported in reference 10. The maximum bending loads in the blade occur in the helicopter mode at the spanwise station of 0.35R. The flapwise bending moments here are about 20,000 in-lb steady and 22,000 in-lb oscillatory for a maximum load of 42,000 in-lb. The maximum chordwise bending moment is somewhat less, but the same moment of 42,000 in-lb is used to insure conservative results. These bending moments are introduced into the structural model by applying a tip load of 430 lb in the flapwise and inplane directions. This method of producing the maximum bending moment at station $0.35R$ also produces a moment distribution in the blade which is a good approximation to the moment distribution reported in the wind tunnel tests of reference 10. The centrifugal load distribution is calculated at the maximum rotational velocity and is a function of the blade weight distribution. The combination of the maximum flapwise and inplane bending moments applied simultaneously with the maximum centrifugal load is the load condition for which the blade designs in this study are substantiated.

Analyses

Structural Analyses

The rotor blade deformations are calculated with a coupled-beam analysis which is based on the theory presented in reference 11. The analysis was originally developed for a single-cell structure, but was extended to treat the case of a two-cell structure such as that used in the present investigation. The single-cell version of the analysis was verified through comparison to an MSC/NASTRAN model in reference 12, and through experimental correlation in reference 4.

A laminate analysis, based on reference 13, is used to determine the material strength margins of safety. The margins are based on Tsai-Hill first-ply failure theory, and are calculated using material design-limit strengths. Material design-limit strengths are obtained by dividing the material ultimate strengths by a factor of 1.5. The use of material design-limit strengths insures linear elastic behavior, and a conservative prediction of the blade strength under the prescribed loads.

Optimization Approach to Blade Design

For this study, the optimization process involves coupling the mathematical optimization analysis CONMIN (ref. 14) to the analyses used to predict deformations and material strength margins of safety. The optimization process requires the definition of an objective function, a set of design variables, and a set of constraints. The optimizer attempts to minimize the objective function through perturbation of the design variables while simultaneously satisfying the prescribed constraints. The objective function and constraints are stated in terms of mathematical expressions which are recalculated for each change in design variable.

The intent of this design study is to achieve twist distributions which improve the performance of the tilt rotor in both hover and forward flight. As discussed previously, this can be accomplished by maximizing the twist deformation for an extension-twist-coupled design at 100 percent rpm. The parameter $\Delta 100$ represents the objective function, and is calculated in the coupled-beam analysis. There are nine design variables needed for the optimization which are defined as follows: three D-spar laminate thicknesses in various sections of the blade, T_{tw}, T_{tr}, and T_{rt}; the laminate thickness in the airfoil skin, T_{sk}; the angle of the plies in the airfoil skin, α_{sk}, and in the spar, α_{sp}; the length of the twisting section, Δx_{tw}; the tip weight, $wtip$; and the additional weight per unit span added to the twisting section, $wnsm$. The only constraint imposed in the present study is that the material strength margin of safety is greater than zero at every point in the structure. However, the design variables affect the material strength margins at different spanwise locations to varying degrees. Thus, it is advantageous to consider the minimum margin of safety at each of the 20 blade segments as a separate constraint. With this selection of constraints, the optimizer can more easily determine how to change the design variables to correct a constraint violation. The material strength margins of safety are calculated in the laminate analysis.

The design variables are limited to realistic values through the use of side constraints. Side constraints can not be violated at anytime in the optimization process. The side constraints applied to the thickness variables are 0.0 in. on the lower bound and 0.3 in. on the upper bound. The laminate angles were bounded between 0° and 45°. The twisting section length was limited to a maximum of 105 in. so that there was a minimum of 22.5 in. of transition section. The minimum length of the twisting section was 15 in. The tip weight was limited to a maximum of 15 lb in one design, 60 lb in a second design, and was not limited in a third design. The 15 lb upper limit keeps the tip weight in the range which is typical of conventional rotor blade designs. The 60 lb limit allows the tip weight to reach an unconventional value, but keeps the weight within a value which can be realistically obtained. The absence of an upper limit on tip weight in the third design will result in the maximum twist deformation at 100 percent rpm even though the design may not be practical. Lastly, the additional running weight added to the twisting section was bounded between 0.0 and 0.3 lb/in.

A second optimization based on the final values of the first optimization is required because of the design variables and assumptions used in this study. In practice, the laminates can be made only in certain thicknesses which are the number of plies multiplied by the thickness per ply available for the material. Also, the laminate layups must be changed in multiples of four plies to maintain the form of $[(\alpha/\alpha+90)_s]_n$, and in multiples of eight plies to maintain the form $[(\alpha/\alpha+90/0/90)_s]_n$. The valid thicknesses could

have been maintained in the first optimization by applying multiple constraints on the thickness design variables. However, it is not desirable to apply multiple constraints on these design variables because large jumps in the thicknesses would result. It is likely that large jumps would impede reaching a global minimum of the objective function. A better approach is to repeat the optimization a second time without thickness design variables. The laminate thicknesses resulting from the first optimization are fixed at the nearest available thicknesses which can be processed for the material. The final design results are obtained by repeating the optimization without the use of thickness design variables. For the remaining design variables, the results of the first optimization are used as initial guesses to the second optimization.

Applications

Design Trends

Some design trends were observed through manual perturbation of the design parameters. The magnitude of twist deformation which can be achieved for an extension-twist-coupled design is highly dependent on the tip weight and blade weight distribution. The maximum twist deformation is obtained within material strength constraints when the twist rate is constant. However, this would only be possible using a tip weight in conjunction with a series of weightless blade segments. Since each segment has weight, the centrifugally generated axial load (and thus the blade twist rate) increases from tip to root. These observations indicate that it is desirable to maximize the use of tip weight and minimize the use of running-weight to obtain a twist rate as close to constant as possible. As the tip weight is increased, the total twist deformation which can be produced within the material strength limits is also increased.

Optimization Results

The optimization approach is used to develop three extension-twist-coupled designs. All three designs are based on the same geometry and assumptions discussed previously except for the upper limit allowed on tip weight as previously mentioned. Design 1 is limited to 15 lb of tip weight which is typical of conventional helicopter blade designs. Design 2 is limited to 60 lb of tip weight which is practical though unconventional, and Design 3 is not limited in tip weight which may result in an impractical design.

Results of the first optimization of each design are listed in Table II. The trend indicated by these results agrees with the trend mentioned previously of increasing twist deformation with increasing tip weight. The thickness parameters reported in Table II are redefined to the nearest processable laminate thickness before beginning the second optimization.

Results of the second optimization are listed in Table III. The trend of increasing twist deformation with increasing tip weight is still evident because the twist deformations of the second optimization are shown to be nearly the same as the twist deformations of the first optimization. Using the twist deformations shown in Table III, the twist distributions for the hover condition were calculated assuming a -42° linear twist in forward flight. The power required to hover was then determined for each design using HOVT. Using these results, the hover performance is plotted as a function of gross weight in figure 7 for the three twist designs and the conventional XV-15 twist. This plot indicates that the differences in horsepower required between the designs are fairly constant with respect to gross weight. Each of the three designs is shown to improve performance over the conventional compromised design. However, Design 3 adds significant weight, about 1200 lb, to the total gross weight which negates any performance improvements it might produce. Design 2 adds about 200 lb to the gross weight which is not negligible, but is not enough to negate its performance improvements.

The hover performance trend with respect to the $\Delta 20$ twist deformation is illustrated in figure 8. This plot shows the change in hover horsepower associated with the three twist designs from that associated with the conventional XV-15 twist, with a negative change in hover horse-

Table II. Extension-Twist-Coupled Designs After First Optimization.

	T_{tw} $(in.)$	T_{tr} $(in.)$	T_{rt} $(in.)$	T_{sk} $(in.)$	α_{sp} $(deg.)$	α_{sk} $(deg.)$	Δx_{tw} $(in.)$	$wtip$ $(lb.)$	$wnsm$ $(lb./in.)$	$\Delta 100$ $(deg.)$
Design 1	.157	.175	.296	.034	15.6	13.8	105.	15.0	.30	19.0
Design 2	.187	.225	.296	.052	15.5	14.2	105.	60.0	.00	27.3
Design 3	.109	.269	.194	.219	13.6	13.0	105.	200.	.00	35.1

Table III. Extension-Twist-Coupled Designs After Second Optimization.

	T_{tw} $(in.)$	T_{tr} $(in.)$	T_{rt} $(in.)$	T_{sk} $(in.)$	α_{sp} $(deg.)$	α_{sk} $(deg.)$	Δx_{tw} $(in.)$	$wtip$ $(lb.)$	$wnsm$ $(lb./in.)$	$\Delta 100$ $(deg.)$	$\Delta 20$ $(deg.)$
Design 1	.154	.176	.286	.044	17.2	16.8	105.	15.0	.30	19.0	6.9
Design 2	.198	.220	.286	.044	15.0	13.3	105.	60.0	.00	27.3	9.8
Design 3	.110	.264	.198	.220	13.2	13.0	105.	201.	.00	35.0	12.8

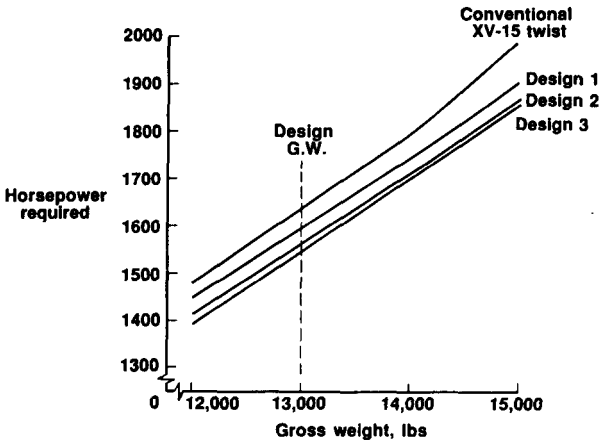

Figure 7. Horsepower required to hover as a function of gross weight.

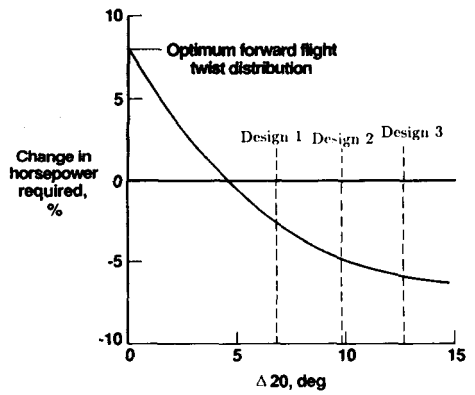

Figure 8. Change in hover horsepower required as a function of twist deformation.

power indicating a performance improvement. A zero value of Δ20 corresponds to a design with no extension-twist coupling so that the twist in hover is the same as the twist in forward flight. The hover performance of the conventional XV-15 twist design is achieved with a Δ20 of about 4.5°. The change in horsepower required is shown to decrease at a diminishing rate until a minimum value of about -6 percent is reached at a Δ20 of approximately 15°. This indicates that for practical designs, with nonlinear twist distributions resulting from extension-twist deformation, a Δ20 of 15° is the optimum twist change for hover which is less twist change than is desired if both twist distributions in hover and forward flight were linear. As discussed previously, the optimum linear twist distributions are -20° and -42° which would require a 22° Δ20 twist deformation. The plot also shows that the hover horsepower-required is improved over the compromised hover horsepower-required by 2.6, 4.8, and 5.8 percent for Design 1, Design 2, and Design 3, respectively.

An example of the change in twist distribution with rotational velocity is presented for Design 1 in figure 9. The

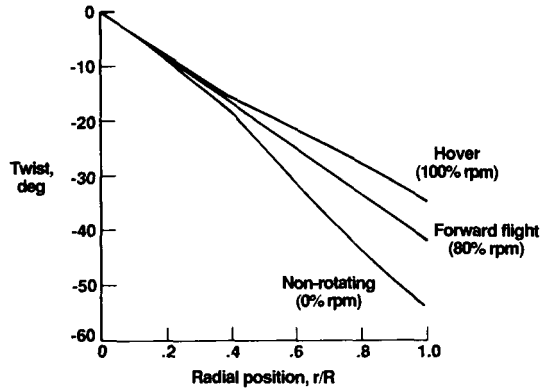

Figure 9. Blade twist distribution of Design 1 in three modes.

twist at 80 percent rpm is shown to be a -42° linear distribution while nonlinear twist distributions are required for the blade at 0 and 100 percent rpm. The figure further shows that the built-in blade twist at 0 rpm has a large negative distribution. As the rotational velocity is increased, the twist distribution moves in a positive direction until it reaches its least negative distribution at 100 percent rpm for the hover condition. As the rotor speed is decreased to 80 percent rpm for forward flight, the twist moves back to a more negative distribution which is linear.

Finite Element Comparison

The bending and twist deformation results calculated with the coupled-beam analysis were compared with an MSC/NASTRAN built-up shell finite-element model for Design 1. The reason for the comparison is that the beam analysis had only been previously verified for single cell structures. The D-spar and airfoil skin comprise a two-cell structure. The finite element model, illustrated in figure 10, used 5640 degrees of freedom and 920 flat-plate quadrilat-

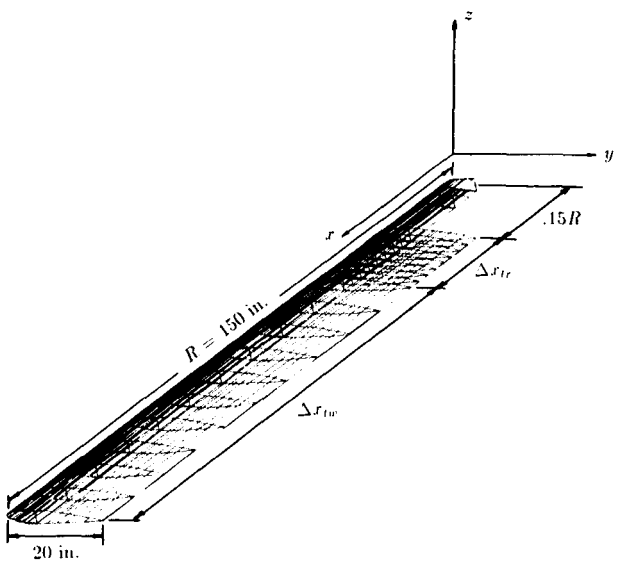

Figure 10. Finite element model of the extension-twist-coupled blade designs.

eral elements to model the structure. The substantiating loads applied in the previous design studies were applied to the finite element model, and the resulting twist and translations are listed in Table IV along with the coupled-beam model results. The finite element and coupled-beam results correlate well with a maximum difference of about 3 percent which indicates that the coupled-beam analysis is adequate for use in this design study.

Table IV. Finite Element and Coupled-Beam Deformations for Design 1.

	Chordwise Translation (*in.*)	Flapwise Translation (*in.*)	Twist, $\Delta 100$ (*deg.*)
Finite Element Model	.466	15.71	19.42
Coupled Beam Model	.433	15.32	19.02

Concluding Remarks

This paper describes the aerodynamic and structural design of a passive blade-twist control concept for tilt rotor aircraft. The linear twist distributions which result in minimum horsepower required were determined for both hover and forward flight. The performance improvement resulting from use of these linear twists instead of the conventional XV-15 twist was also determined. Three extension-twist-coupled rotor blades were designed with various amounts of tip weight. Design 1 had 15 lb of tip weight which is typical of conventional helicopter rotor blades. Design 2 had 60 lb of tip weight which is much more than that used in conventional designs, but can be realistically obtained. Design 3 was not limited in tip weight which resulted in the maximum twist deformation although the weight increase made the design impractical. All three designs were obtained by optimizing for maximum twist deformation subject to material strength constraints. The twist change available for each design was used to determine its hover twist distribution and the resulting hover performance.

The performance benefits predicted for use of the aerodynamically-optimum linear twists instead of the conventional XV-15 twist were significant, with 6.1 percent horsepower savings in hover and 6.5 percent horsepower savings in forward flight. All three extension-twist-coupled designs resulted in 6.5 percent horsepower improvements in forward flight because the optimum linear twist was obtained. In increasing the rotor speed for the hover condition, significant amounts of twist change were developed which resulted in nonlinear twist distributions. The hover twist distributions resulted in significant improvements to hover performance with savings of 2.6, 4.8, and 5.8 percent for Design 1, Design 2, and Design 3, respectively. Design 3 increased the gross weight substantially which makes that design impractical. Designs 1 and 2, however, are practical and result in significant improvements in horsepower required in both hover and forward flight. These results indicate that the passive blade-twist control concept is viable and can enhance current tilt rotor performance.

References

1. McVeigh, M.A., Rosenstein, H.J. and McHugh, F.J.: Aerodynamic Design of the XV–15 Advanced Composite Tilt Rotor Blade. 39th Annual Forum, American Helicopter Soc., 1983.

2. Johnson, W., Lau, B.H., and Bowles, J.V.: Calculated Performance, Stability, and Maneuverability of High Speed Tilting Proprotor Aircraft. *Vertica*, Vol. 11, 1987.

3. Bauchau, O.A., Loewy, R.G., and Bryan, P.S.: An Approach to Ideal Twist Distribution in Tilt Rotor VSTOL Blade Designs. AHS 39th Annual Forum Proceedings, May 1983.

4. Nixon, M.W.: Extension–Twist Coupling of Circular Tubes with Application to Tilt Rotor Blade Design. AIAA Paper 87-0772, 28th Structures, Structural Dynamics and Materials Conference, Monterey, CA, April 1987.

5. McCormick, B. W., Jr.: *Aerodynamics of V/STOL Flight.* Academic Press, c.1967.

6. Johnson, W.: A Comprehensive Analytical Model of Rotorcraft Aerodynamics and Dynamics. NASA TM 81182, 81183, 81184, 1980.

7. Gessow, A., and Myers, G.C.: *Aerodynamics of the Helicopter.* Frederick Ungar Publishing Co., c.1952.

8. Walsh, J.L., Bingham, G.J., and Riley, M.F.: Optimization Methods Applied to the Aerodynamic Design of Helicopter Rotor Blades. AIAA Paper 85-0644, 26th Structures, Structural Dynamics, and Materials Conference, Orlando, FL, April 1985.

9. *Military Specification – Structural Design Requirements, Helicopters.* MIL-S-8698, Apr. 20, 1981.

10. Bell Helicopter Company: Advancement of Proprotor Technology – Wind Tunnel Test Results. NASA CR-114363, Sept. 1971.

11. Rehfield, L. W.: Design Analysis Methodology for Composite Rotor Blades. Seventh DoD/NASA Conference on Fibrous Composites in Structural Design, Denver, CO, June 1985.

12. Hodges, R.V., Nixon, M.W., and Rehfield, L.W.: Comparison of Composite Rotor Blade Models: A Coupled–Beam Analysis and an MSC/NASTRAN Finite-Element Model, NASA TM 89024, AVSCOM TM 87-B-2, 1987.

13. Jones, R.M.:*Mechanics of Composite Materials.* McGraw-hill, 1975.

14. Vanderplaats, G. N.: CONMIN – A FORTRAN Program for Constrained Function Minimization, User's Manual. NASA TM X-62 282, August 1973.

Standard Bibliographic Page

1. Report No.	2. Government Accession No.	3. Recipient's Catalog No.
NASA TM-100583 AVSCOM TM 88-B-010		

4. Title and Subtitle	5. Report Date
Improvements to Tilt Rotor Performance Through Passive Blade Twist Control	April 1988
	6. Performing Organization Code
7. Author(s)	8. Performing Organization Report No.
Mark W. Nixon	
9. Performing Organization Name and Address Aerostructures Directorate USAARTA-AVSCOM NASA, Langley Research Center Hampton, VA 23665-5225	10. Work Unit No. 505-63-51-01
	11. Contract or Grant No.
12. Sponsoring Agency Name and Address National Aeronautics and Space Administration Washington, D.C. 20546-0001 and U. S. Army Aviation Systems Command, St. Louis, MO 63120-1798	13. Type of Report and Period Covered Technical Memorandum
	14. Sponsoring Agency Code

15. Supplementary Notes

Mark W. Nixon: Aerostructures Directorate, USAARTA-AVSCOM
The use of trademarks or names of manufacturers in this report is for accurate reporting and does not constitute an official endorsement, either expressed or implied, of such products or manufacturers by the National Aeronautics & Space Admin.

16. Abstract

A passive blade twist control is presented in which the twist distribution of a tilt rotor blade is elastically changed as a function of rotor speed. The elastic twist deformation is used to achieve two different blade twist distributions corresponding to the two rotor speeds used on conventional tilt rotors in hover and forward flight. By changing the blade twist distribution, the aerodynamic performance can be improved in both modes of flight. The concept presented in this paper obtains a change in twist distribution with extension-twist-coupled composite blade structure. This investigation first determines the linear twists which are optimum for each flight mode. Based on the optimum linear twist distributions, three extension-twist-coupled blade designs are developed using coupled-beam and laminate analyses integrated with an optimization analysis. The designs are optimized for maximum twist deformation subject to material strength limitations. The aerodynamic performances of the final designs are determined which show that the passive blade twist control concept is viable, and can enhance conventional tilt rotor performance.

17. Key Words (Suggested by Authors(s))	18. Distribution Statement
Anisotropy Composite Materials Elastic Tailoring Extension-twist coupling Rotor Blades Tilt Rotors	Unclassified - Unlimited Subject Category 39

19. Security Classif.(of this report)	20. Security Classif.(of this page)	21. No. of Pages	22. Price
Unclassified	Unclassified	10	A02

For sale by the National Technical Information Service, Springfield, Virginia 22161